Capacitance Extraction of 3-D Conductor Systems in Dielectric Media with high Permittivity Ratios

Johannes Tausch and Jacob White

Abstract— **The recent development of fast algorithms for solving dense linear systems generated by boundary-element methods, such as the multipole-accelerated algorithms, has renewed interest in improving integral formulations for problems in electromagnetics. In this paper we describe a perturbation formulation for the problem of computing electrostatic capacitances of multiple conductors embedded in multiple dielectric materials. Unlike the commonly used equivalent charge formulation, this new approach insures that the capacitances are computed accurately even when the permittivity ratios of the dielectric materials are very large. Computational results from a three-dimensional multipole-accelerated algorithm based on this approach are presented. The results show that the accuracy of this new approach is not only superior to the equivalent charge formulation, the accuracy is nearly independent of the permittivity ratios.**

I. Introduction

The self and coupling capacitances associated with integrated circuit interconnect and packaging are becoming increasingly important in determining final circuit performance and reliability. However, accurate estimation of these capacitances involves analyzing innately three-dimensional structures with dielectric materials surrounding conductors in a complicated fashion. Integrated circuits, for example, have multiple layers of polysilicon or metal conductors, separated by conformal or space-filling dielectrics. Also, packaging and off-chip interconnection problems often involve connectors passing through several plastic or ceramic dielectrics.

Among the techniques for capacitance calculation methods in homogeneous media, the integral equation method, or moment method [1], is generally preferred as only surfaces need to be discretized. When combined with acceleration schemes like the fast multipole method, the analysis of very complex 3-D structures become computationally inexpensive [2].

For conductor systems in layered media, the integral equation method is altered by using modified Green's functions. However, the Green's function gets increasingly more complicated with the number of layers [3],[4] and multipole acceleration schemes become much harder to implement [5].

A simpler approach that applies to arbitrary geometries of conductors and dielectric interfaces is the equivalent charge formulation (ECF) [6]. This technique includes polarization charges on the dielectric interfaces in addition to the conductor charges, thus requiring the solution of a larger matrix equation. However, the approach only involves free-space Green's functions and thus the arising linear system can easily be sparsified with the fast multipole method [7].

It is well known that the ECF can result in very poor numerical approximations of capacitances when the ratios of the involved permittivities are large, see e.g. [8]. For such problems, Galerkin methods are far more accurate than centroid collocation [9], but even Galerkin methods will fail for sufficiently high permittivity ratios.

This paper gives an explanation why any numerical scheme discretizing the equivalent charge formulation will fail for high permittivity ratios. We will demonstrate that in this case the approximation becomes poor because the conductor charge is much smaller than the polarization charge. Therefore the quantity of interest, the conductor charge, will have large relative errors resulting in large errors of the computed capacitances.

To avoid simultaneously solving for unknowns over a many orders of magnitude range, the method described below decomposes the original problem into two problems which are solved consecutively. The first problem corresponds to replacing the finite permittivity dielectric with an infinite permittivity dielectric and involves only large-scale unknowns on the interface. To account for the finite permittivity a perturbation equation is solved on both surfaces which only involves small-scale unknowns.

Sections II and III briefly review the equivalent charge formulation as well as some issues for calculating capacitance matrices of multiconductor systems

This work is supported by NSF contract ECS-9301-189 and the DARPA MURI program

with dielectric materials. The numerical problems that arise for the equivalent charge formulation in the case of high permittivity ratios are described in Section IV. In Section V a modification of the existing method is presented which avoids the difficulties of the equivalent charge formulation. The technique is extended to the multiple conductor case in Section VI and its utility is demonstrated in Section VII by applying our multipole-accelerated implementation of the algorithm to complex multiconductor systems.

II. Boundary Integral Formulation

In inhomogeneous media with permittivity $\varepsilon(x)$ the electrostatic potential ϕ and the electric field $\nabla\phi$ satisfy the boundary value problem

$$\begin{array}{rcll} \nabla^2\phi &=& 0 & \text{in } \mathbb{R}^3 \setminus S\,, \\ \phi &=& u & \text{on } S_c\,, \\ \phi^+ &=& \phi^- & \text{on } S_d\,, \\ \varepsilon^+ \frac{\partial\phi^+}{\partial n} &=& \varepsilon^- \frac{\partial\phi^-}{\partial n} & \text{on } S_d\,, \\ \phi &=& \mathcal{O}(\frac{1}{|x|}) & \text{as } |x| \to \infty\,. \end{array} \tag{1}$$

Here S_c denotes the union of the conductor surfaces, u denotes the given potential on the conductors, S_d is the union of the dielectric interfaces, n is the normal to S_d, and $\phi^\pm = \phi(x \pm 0n)\,, \varepsilon^\pm = \varepsilon(x \pm 0n)$ and $S = S_c \cup S_d$.

Since (1) is an exterior problem, it is advantageous for numerical calculations to cast the differential equation into a boundary integral equation. This is a common approach in electrostatics because the charge density can be calculated directly with this approach. To obtain an integral formulation, write the potential ϕ as the superposition of potentials due to the conductor charge σ_c and the polarization charge on the interface σ_d. In operator notation this becomes

$$\phi(x) = V_c\sigma_c(x) + V_d\sigma_d(x)\,, \quad x \in \mathbb{R}^3\,. \tag{2}$$

Here V_c and V_d denote the single-layer potentials on the boundary surfaces S_c and the interfaces S_d, respectively, defined by

$$V_c\sigma_c(x) = \int_{S_c} G(x,x')\,\sigma_c(x')\,dS_{x'}\,, \quad x \in \mathbb{R}^3\,,$$

and

$$V_d\sigma_d(x) = \int_{S_d} G(x,x')\,\sigma_d(x')\,dS_{x'}\,, \quad x \in \mathbb{R}^3\,.$$

The kernel $G(x,x')$ is the free-space Green's function for the Laplace operator in three dimensions

$$G(x,x') = \frac{1}{4\pi}\frac{1}{|x-x'|}\,. \tag{3}$$

Note that the conductor charge σ_c consists of free charges in the conductor and polarization charges in the dielectric material. For the capacitance only the free charges are important. They are linked to the conductor charge by

$$\sigma_f = \varepsilon^+\sigma_c\,.$$

The potential defined in (2) satisfies Laplace's equation, is continuous throughout the three-space and decays like $1/|x|$. In order to solve the boundary value problem (1), the potential must also satisfy the boundary conditions on the conductors as well as the continuity condition on the interfaces. The latter conditions will lead to a system of integral equations for the densities σ_c and σ_d. For that we must consider the limiting values of $\phi(x)$ defined by (2) as $x \to S$. It is well-known that the potential is continuous, but its normal derivative is not continuous across the surface, see, e.g, [10]. In particular, the following jump relation holds on S_d

$$\frac{\partial\phi^\pm}{\partial n}(x) = K'_c\sigma_c(x) + \left(\mp\frac{1}{2} + K'_d\right)\sigma_d(x)\,, \quad x \in S_d\,. \tag{4}$$

Here the operator K'_c denotes the normal derivative on the dielectric interface due to the conductor charge and is defined by

$$K'_c\sigma_c(x) = \int_{S_c} \frac{\partial}{\partial n_x} G(x,x')\,\sigma_c(x')\,dS_{x'}\,, \quad x \in S_d\,.$$

The operator K'_d is defined similarly for charges on the interfaces.

Combining (2) and (4) with the boundary conditions of (1), the following system of integral equations for the densities σ_c and σ_d can be derived

$$\begin{array}{rcll} V_c\sigma_c(x) + V_d\sigma_d(x) &=& u(x)\,, & x \in S_c \\ K'_c\sigma_c(x) + \left(\frac{1}{2\lambda} + K'_d\right)\sigma_d(x) &=& 0\,, & x \in S_d\,. \end{array} \tag{5}$$

The parameter λ is given by

$$\lambda = \frac{\varepsilon^- - \varepsilon^+}{\varepsilon^- + \varepsilon^+}\,. \tag{6}$$

The orientation of the surface normal in equations (1) and (4) is arbitrary. We will use the convention that the normal of S_d points into the domain of the lower permittivity, this will ensure that $0 < \lambda < 1$.

Subtracting the jump relations (4) for both sides of the surface yields the important relation between the charge density and the jump in the normal derivative of the potential

$$\sigma = \frac{\partial \phi^-}{\partial n} - \frac{\partial \phi^+}{\partial n} . \tag{7}$$

Formulation (5) has appeared previously in the literature [6], and is usually referred to as the equivalent charge formulation.

In the following we will also make use of another relation between the charge density and the potential of the capacitance problem. Namely, for the solution ϕ of (1) and σ_c of (5)

$$\int_{\mathbb{R}^3} \varepsilon \, |\nabla \phi|^2 = \int_{S_c} \varepsilon \sigma u \tag{8}$$

holds. This formula follows by applying Green's first identity to every connected component of $\mathbb{R}^3 \setminus S$.

III. Capacitance Matrices

Since the potential on each conductor in an m conductor problem must be constant, $u(x)$ in (5) can be associated with a vector $p \in \mathbb{R}^m$. Specifically

$$u(x) = p_i, \quad x \in S_{c_i}, \tag{9}$$

where S_{c_i} is the surface of the i^{th} conductor. Then, given $u(x)$ associated with a vector p, let $q \in \mathbb{R}^m$ be the vector of net free charges on each conductor as in

$$q_i = \int_{S_{c_i}} \varepsilon \sigma_c. \tag{10}$$

The capacitance matrix, $\mathbf{C} \in \mathbb{R}^{m \times m}$, summarizes the relation between the conductor potentials and conductor charges,

$$\begin{bmatrix} C_{1,1} & ,\ldots, & C_{1,m} \\ \vdots & \vdots & \vdots \\ C_{m,1} & ,\ldots, & C_{m,m} \end{bmatrix} \begin{bmatrix} p_1 \\ \vdots \\ p_m \end{bmatrix} = \begin{bmatrix} q_1 \\ \vdots \\ q_m \end{bmatrix} . \tag{11}$$

To compute the complete capacitance matrix, it is necessary to solve (5) m times using u's associated with m linearly independent p vectors. An obvious choice for the p vectors is to choose them equal to the m unit vectors. For example, if $p^{(i)}$ is the i^{th} unit vector and $q^{(i)}$ is the resulting vector of conductor charges, then $q^{(i)}$ is the i^{th} column of $\mathbf{C}$. Even though choosing the p vectors to be unit vectors leads to a simple relation between the computed q vectors and columns of the capacitance matrix, we will show in a subsequent section that unit vectors are not always the best choice.

For the case of a general set of linearly independent p vectors,

$$\begin{bmatrix} C_{1,1} & ,\ldots, & C_{1,m} \\ \vdots & \vdots & \vdots \\ C_{m,1} & ,\ldots, & C_{m,m} \end{bmatrix} \begin{bmatrix} \vdots & ,\ldots, & \vdots \\ p^{(1)} & ,\ldots, & p^{(m)} \\ \vdots & ,\ldots, & \vdots \end{bmatrix}$$

$$= \begin{bmatrix} \vdots & ,\ldots, & \vdots \\ q^{(1)} & ,\ldots, & q^{(m)} \\ \vdots & ,\ldots, & \vdots \end{bmatrix}$$

and therefore the capacitance matrix can be determined from

$$\begin{bmatrix} C_{1,1} & ,\ldots, & C_{1,m} \\ \vdots & \vdots & \vdots \\ C_{m,1} & ,\ldots, & C_{m,m} \end{bmatrix}$$

$$= \begin{bmatrix} \vdots & ,\ldots, & \vdots \\ q^{(1)} & ,\ldots, & q^{(m)} \\ \vdots & ,\ldots, & \vdots \end{bmatrix} \begin{bmatrix} \vdots & ,\ldots, & \vdots \\ p^{(1)} & ,\ldots, & p^{(m)} \\ \vdots & ,\ldots, & \vdots \end{bmatrix}^{-1} .$$

IV. High Permittivity Ratios

Typically, system (5) is discretized with piecewise constant collocation. Numerical experience shows that the error of the approximated capacitances grow rapidly as the ratio of the permittivities increases, see e.g. [8]. In the same article it is proposed to employ the Galerkin method for the discretization of (5). Even though the Galerkin scheme improves the approximation, the method produces inaccurate results if the permittivity ratio becomes very high. In the following we will explain why this happens.

To simplify the exposition, we consider a conductor raised to one volt which is embedded in a dielectric material, as depicted in Figure 1. The multiconductor case will be discussed in Section VI.

To study large permittivities set $\varepsilon_0 = 1$ and let $\varepsilon_1 \to \infty$, which is equivalent to letting λ in (6) approach 1. Thus integral equation (5) reduces to

$$\begin{aligned} V_c \sigma_{c,\infty}(x) + V_d \sigma_{d,\infty}(x) &= 1\,, \quad x \in S_c \\ K_c' \sigma_{c,\infty}(x) + \left(\tfrac{1}{2} + K_d'\right) \sigma_{d,\infty}(x) &= 0\,, \quad x \in S_d\,. \end{aligned} \tag{12}$$

The behavior of the densities $\sigma_{c,\infty}$ and $\sigma_{d,\infty}$ can be seen by looking at the potential

$$\phi_\infty = V_c \sigma_{c,\infty} + V_d \sigma_{d,\infty}$$

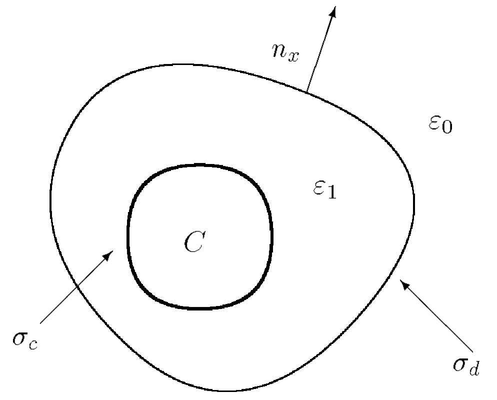

Fig. 1. Inclusion of the conductor C into a dielectric material with permittivity ε_1. The permittivity of the free space is ε_0.

generated by the solution of (12). From this integral equation we see that $\phi_\infty = 1$ on S_c and that $\partial\phi_\infty^-/\partial n = 0$ on S_d. Since ϕ_∞ satisfies Laplace's equation, the potential is constant within the ε_1-material and the conductor. By (7) the conductor charge, $\sigma_{c,\infty}$, vanishes. Since the potential is also 1 on the dielectric interface, the polarization charge satisfies the integral equation

$$V_d\sigma_{d,\infty}(x) = 1\,, \quad x \in S_d\,. \tag{13}$$

Physically, the $\varepsilon_1 \to \infty$ limit implies that the dielectric material is acting like a conductor. Hence all charges must be located on the dielectric interface and the conductor density must vanish. Equation (13) is equivalent to calculating the capacitance of the structure where the dielectric material has been replaced by a conductor. Thus the original problem which was posed on S_c and S_d is reduced to a problem posed on S_d only. Moreover, the capacitance of this problem is given by

$$\mathbf{C}_\infty = \int_{S_d} \sigma_{d,\infty}\, dS\,.$$

Now consider the densities σ_c, σ_d in the equivalent charge formulation (5) for large, but finite ε_1. Since the solution of the equivalent charge formulation depends continuously on the parameter λ, it is clear that σ_c is small compared to σ_d, because σ_c converges to zero whereas σ_d converges to the non-zero charge $\sigma_{d,\infty}$.

When solving (5) numerically, the discretization error will be distributed evenly over both surfaces resulting in large relative errors of the conductor surface charge. This destroys the accuracy of the capacitance based on (10), because the inaccurately computed charge density on S_c will be multiplied by ε_1 to calculate the capacitance in (10) and any discretization error will be multiplied by the same factor. On the other hand, the exact value of $\mathbf{C}$ converges to $\mathbf{C}_\infty$. This can be seen by integrating the second equation in (5) over the interface S_d. By Gauss's law, we have $\int_{S_d} K_c'\sigma_c = -\int_{S_c}\sigma_c$ and $\int_{S_d} K_d'\sigma_d = -1/2\int_{S_d}\sigma_d$. Hence,

$$\mathbf{C} = \int_{S_c} \varepsilon_1\sigma_c = \varepsilon_1\Big(\frac{1}{2\lambda} - \frac{1}{2}\Big)\int_{S_d}\sigma_d \to \mathbf{C}_\infty\,. \tag{14}$$

Thus the discretization error of $\mathbf{C}_\lambda$ grows linearly with ε_1 whereas the exact value remains finite in the limit of $\varepsilon_1 \to \infty$.

V. The Perturbation Approach

The major numerical difficulty associated with high permittivity ratios is that the small-scale conductor charge is used to calculate the capacitance. For a single conductor, the self-capacitance could also be calculated via (14) using the polarization charge and thus avoiding large relative discretization errors. However, this idea does not provide an accurate approximation of the conductor charge density and does not extend to multiconductor systems. Instead, we describe here a perturbation technique which allows for accurate estimates of the conductor charge density and extend the approach to the multiconductor case in the following section.

The idea of the perturbation approach (PA) is to set up the potential as the combination of ϕ_∞, the potential generated by $\varepsilon_1 = \infty$, and the correction $\tilde\phi$ accounting for the finite permittivity

$$\phi(x) = \phi_\infty(x) + \tilde\phi(x)\,. \tag{15}$$

As was shown above, the potential ϕ_∞ results only from the charge $\sigma_{d,\infty}$ on the interface, which is given by integral equation (13). This is a capacitance problem in homogeneous media and can be solved numerically to high accuracy [2], [9].

The perturbation $\tilde\phi$ is set up as a superposition of charges on the conductor surface and the dielectric interface, similar to the definition of the potential in (2)

$$\tilde\phi(x) = V_c\tilde\sigma_c(x) + V_d\tilde\sigma_d(x)\,. \tag{16}$$

Substituting (16) into (1), one obtains a new set of boundary conditions for the perturbation $\tilde\phi$

$$\begin{aligned} \tilde\phi(x) &= 0\,, & x &\in S_c \\ \varepsilon^-\frac{\partial\tilde\phi^-}{\partial n}(x) - \varepsilon^+\frac{\partial\tilde\phi^+}{\partial n}(x) &= -\varepsilon^+\sigma_{d,\infty}(x)\,, & x &\in S_d\,. \end{aligned} \tag{17}$$

The second equation holds because ϕ_∞ is constant within the dielectric material and hence $\partial\phi_\infty^-/\partial n = 0$ and $\partial\phi_\infty^+/\partial n = -\sigma_{d,\infty}$ by the jump relation (7).

These boundary conditions yield, very much in the same way as for (5), the following system of integral equations for the perturbation charges $\tilde{\sigma}_c$ and $\tilde{\sigma}_d$

$$\begin{array}{rcll} V_c\tilde{\sigma}_c(x) + V_d\tilde{\sigma}_d(x) & = & 0 & x \in S_c \\ K_c'\tilde{\sigma}_c(x) + (\frac{1}{2\lambda} + K_d')\tilde{\sigma}_d(x) & = & \frac{\lambda-1}{2\lambda}\sigma_{\infty,d}(x) & x \in S_d\,. \end{array} \tag{18}$$

Since the potential ϕ_∞ is generated only by charges on the dielectric interface, it follows that $\tilde{\sigma}_c = \sigma_c$. Moreover, the capacitance in (10) reduces to an integral over the perturbation charge

$$\mathbf{C} = \varepsilon_1 \int_{S_c} \tilde{\sigma}_c \, dS\,. \tag{19}$$

System (18) has the same operator on the left hand side as the original system (5), only the right hand side has changed. This is the key observation. The right hand side scales like $\mathcal{O}(1/\varepsilon_1)$ as $\varepsilon_1 \to \infty$. Hence, by linearity, we see that $\tilde{\sigma}_c$ and $\tilde{\sigma}_d$ are both $\mathcal{O}(1/\varepsilon_1)$ and therefore there is no different scaling in the solution of equation (18).

By the same argument the error due to discretizing (18) scales like $\mathcal{O}(1/\varepsilon_1)$ for a fixed meshwidth. Hence the error of the capacitance in (19) can be bounded independently of the permittivity ε_1.

The perturbation approach for calculating capacitances of structures involving dielectrics with high permittivities is summarized below.

1. Solve problem (13) on the interface for $\sigma_{d,\infty}$.
2. Solve the perturbation equation (18).
3. Calculate the capacitance via formula (19).

VI. Multiconductor Systems

The technique described above for a single conductor can be generalized to structures consisting of multiple conductors with arbitrary geometries. We illustrate the method with the structure shown in Figure 2.

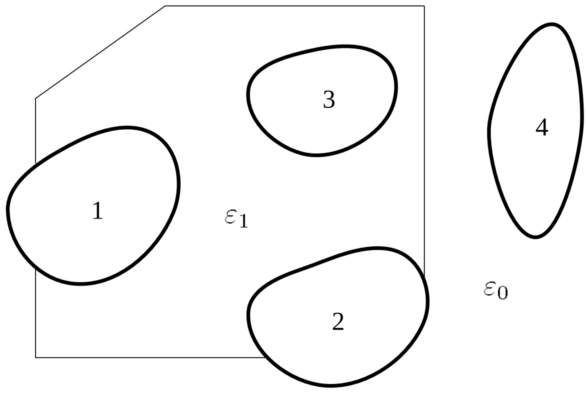

Fig. 2. Multiconductor system. For clarity, conductor surfaces are shown curved, whereas dielectric interfaces are polygonal.

For the limit $\varepsilon_1 \to \infty$ there are two cases that exhibit different behavior of the charge density.

Case 1. Conductors 1, 2 and 3 have the same potential, $p_1 = p_2 = p_3 = p_0$. This case is quite similar to the single conductor case. In the limit $\varepsilon_1 \to \infty$ we have on the interface

$$\frac{\partial\phi^-}{\partial n} \to 0 \tag{20}$$

and it can be seen from (1) that the potential in the dielectric medium approaches the constant value p_0. Thus the field in the dielectric vanishes and a more careful analysis shows that

$$\int_D |\nabla\phi|^2 = \mathcal{O}(1/\varepsilon_1)\,, \tag{21}$$

where D denotes the region of the ε_1-material. From Green's first identity (8) it follows that for $\mathbf{p} = [p_0, p_0, p_0, p_4]^T$, $p_4 \in \mathbb{R}$

$$\frac{\mathbf{p}^T\mathbf{C}\mathbf{p}}{\mathbf{p}^T\mathbf{p}} = \mathcal{O}(1)\,, \quad \text{as } \varepsilon_1 \to \infty\,.$$

Case 2. Conductors 1, 2 and 3 have different potentials. In this case the potential within the dielectric material cannot approach a constant, and

$$\int_D |\nabla\phi|^2 = \mathcal{O}(1)\,, \quad \text{as } \varepsilon_1 \to \infty\,, \tag{22}$$

and thus in view of Green's first identity

$$\frac{\mathbf{p}^T\mathbf{C}\mathbf{p}}{\mathbf{p}^T\mathbf{p}} = \mathcal{O}(\varepsilon_1)\,.$$

Letting $\varepsilon_1 \to \infty$ in the first case corresponds to replacing the dielectric material by a conductor, whereas the limit has no physical meaning for the second case. In fact, as $\varepsilon_1 \to \infty$ the potential energy for the second case approaches infinity.

If the charge density for the first case is calculated via the equivalent charge formulation (5), then the same scaling problem occurs as in the single conductor case. Because of (7) and (20), the charge density on the conductor surfaces facing the ε_1-material scales like $1/\varepsilon_1$ whereas the polarization charge σ_d approaches a non-zero distribution. Again, the different scaling in the equivalent charge formulation can be avoided with the perturbation approach.

The first step is to calculate the charge distribution associated with replacing the ε_1-material by a conductor. For this, remove all ε_1-conductor surfaces. For the structure shown in Figure 2, conductor 3 and parts of conductors 1 and 2 have to be removed. Furthermore, the interface panels are replaced by conductor panels. The result is a capacitance problem in a homogeneous medium.

As in the single conductor case, the perturbation charge is obtained by superposition as in (15). The result is a system of the form (18) whose right hand side and solution scale like $1/\varepsilon_1$.

If the conductors in the ε_1-material have different potentials, there is no bad scaling in (5), because in the $\varepsilon_1 \to \infty$ limit charges must remain on the ε_1-conductor surfaces to maintain a non-constant potential in the dielectric material. Thus the charge density can be calculated directly via (5).

Now consider calculating one column of the capacitance matrix of a multiconductor system by raising a conductor to one volt while grounding the others. For the structure of Figure 2 one could apply the perturbation approach to calculate column $\mathbf{C}_{4,j}$ and the equivalent charge approach to obtain all other entries. Although this approach avoids different scales in the calculation each column, there is still a problem. Namely, if $\mathbf{C}$ is used to determine the net charge on the conductors for the potential distribution $\mathbf{p} = [1, 1, 1, 0]^T$, then resulting charge vector has bad scaling. Hence the discretization error will scale like ε_1, whereas the charge will approach a finite limit, resulting in large relative errors.

To avoid this problem calculate $\mathbf{C}$ in a different coordinate system. For this let $\mathbf{P}_-$ be the matrix whose columns consist of an orthonormal basis of vectors $\mathbf{p}$ whose product $\mathbf{p}^T\mathbf{C}\mathbf{p}/\mathbf{p}^T\mathbf{p}$ remains bounded as $\varepsilon_1 \to \infty$. Furthermore, denote by $\mathbf{P}_+$ the corresponding matrix for the orthogonal complement. The matrices $\mathbf{P}_\pm$ can be determined easily from the problem geometry. For our example we have

$$\mathbf{P}_- = \begin{bmatrix} \frac{1}{\sqrt{3}} & 0 \\ \frac{1}{\sqrt{3}} & 0 \\ \frac{1}{\sqrt{3}} & 0 \\ 0 & 1 \end{bmatrix} \quad \text{and } \mathbf{P}_+ = \begin{bmatrix} \frac{1}{\sqrt{2}} & \frac{1}{\sqrt{6}} \\ \frac{-1}{\sqrt{2}} & \frac{1}{\sqrt{6}} \\ 0 & \frac{-2}{\sqrt{6}} \\ 0 & 0 \end{bmatrix} .$$

Furthermore, set $\mathbf{Q}_\pm = \mathbf{C}\mathbf{P}_\pm$, $\mathbf{P} = [\mathbf{P}_-, \mathbf{P}_+]$ and $\mathbf{Q} = [\mathbf{Q}_-, \mathbf{Q}_+]$. By linearity of the capacitance problem, the entry $\mathbf{Q}_{i,k}$ is the net charge on conductor i when the potential on the conductors is given by the k-th column of $\mathbf{P}$. Thus $\mathbf{Q}_-$ scales like $\mathcal{O}(1)$ and can be calculated stably using the perturbation approach. The matrix $\mathbf{Q}_+$ contains the part of the capacitance matrix that scales like $\mathcal{O}(\varepsilon_1)$ and can be determined directly by the equivalent charge formulation.

Since the matrix $\mathbf{P}$ is orthonormal $\mathbf{P}^{-1} = \mathbf{P}^T$ and

$$\mathbf{C}' = \mathbf{P}^T\mathbf{C}\mathbf{P} = \mathbf{P}^T\mathbf{Q}$$

is a similarity transform of $\mathbf{C}$. The capacitance matrix matrix can be determined by calculating the matrix $\mathbf{Q}$ first and then recovering $\mathbf{C}$ from

$$\mathbf{C} = \mathbf{P}\mathbf{C}'\mathbf{P}^T = \mathbf{Q}\mathbf{P}^T .$$

VII. Results

To demonstrate the accuracy and stability of the perturbation approach (PA) described in this article, we compare the capacitances obtained by the PA, ECF and other approaches for several structures and permittivity ratios. While the first three examples illustrate the solution behavior for simple geometries, the last two examples are included to demonstrate that the PA can be useful for more realistic and complex structures.

The problems were discretized with piecewise constant collocation and the arising linear systems were solved using the iterative solver GMRES. To accelerate the matrix-vector products, the fast multipole algorithm was applied, [11], [12]. Our code is based on the package `FASTCAP` [2] with some modifications to calculate the normal derivatives of the potential for the interface condition. The results are displayed dimension-free, that is, $\varepsilon_0 = 1$.

A. Coated Sphere

In the first example we approximate the capacitance of the unit radius spherical conductor which is covered by a concentric unit thick coating with the discretization as shown in Figure 3.

Because of the spherical geometry, the analytic value of the capacitance is known. The same discretization into 1536 panels was used to approximate the capacitance with the equivalent charge formulation and by the perturbation method for a wide range of permittivity ratios.

Figure 4 compares the discretization errors obtained from both formulations. As it can be seen from this plot, the equivalent charge approach gives enormous discretization errors for high permittivity ratios,

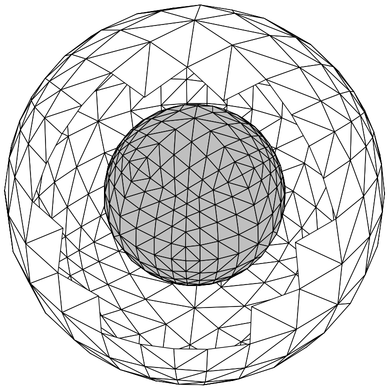

Fig. 3. The coated sphere. Some of the interface panels have been removed to show the inner conductor surface panels.

whereas the the error of the perturbation approach remains small, even when $\varepsilon_1 \to \infty$.

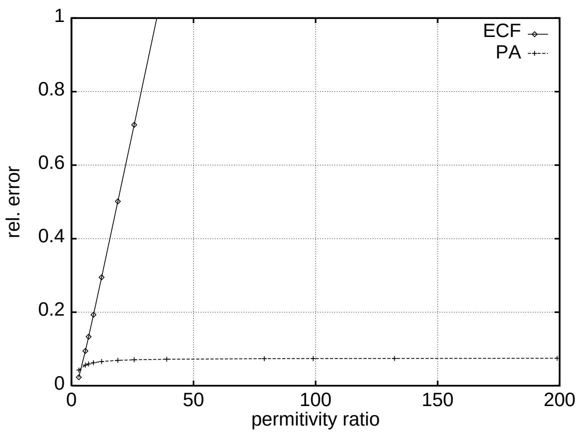

Fig. 4. Relative errors of the capacitance as calculated by the equivalent charge formulation and the modified formulation. Coated sphere example. The exact value of the capacitance varies between 18 and 25.

The condition number for a fixed discretization is bounded as the permittivity ratio is increased. This is true for both formulations. The reason is that the equivalent charge formulation (5) converges in the limit $\lambda \to 1$ to the well-posed integral equation (12). As a result, the number of GMRES iterations to solve the discretized linear systems is independent of the permittivity. This is demonstrated for the coated sphere in Table I. For the other structures the iterative method took more steps to converge, but showed the same independence of the permittivity. This again makes clear that the accuracy problem of the equivalent charge formulation is not ill-conditioning, but a scaling problem.

ε_1	2	5	10	20	50	100	1,000
ECF	7	7	7	7	7	7	7
PA	8	8	8	8	8	8	8

TABLE I

Number of GMRES iterations required to solve the equivalent charge formulation and the perturbation equation for the coated sphere problem.

B. Two Spheres in a Dielectric Medium

The second structure consists of two spheres in an ellipsoidal dielectric medium. The defining equations for the conductors and the interface are

$$\begin{aligned} x_1^2 + (x_2 + \frac{3}{4})^2 + x_3^2 &= \frac{1}{4}, \\ (x_1 - \frac{1}{5})^2 + (x_2 - \frac{4}{5})^2 + (x_3 - \frac{1}{5})^2 &= \frac{1}{3}, \\ x_1^2 + x_2^2 + \frac{9}{4}x_3^2 &= \frac{9}{4}, \end{aligned}$$

respectively. As there is no closed-form solution for this problem, we investigate the behavior of the numerical approximation for different mesh refinements. To make the differences between conductors at equal and different potentials clear, we display in Table II the computed net free charges for potential vectors $p = [1, 1]^T$ and $p = [1, -1]^T$.

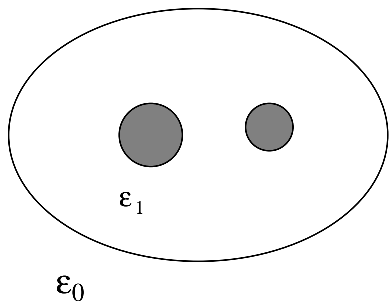

Fig. 5. Two Spheres in a Dielectric Medium

In the equal potential case there is a significant difference in the convergence behavior of the ECF and the PA. For all permittivities calculated, the net-charges obtained using the PA and the $2,304$ panel grid are within five to six percent of the corresponding values obtained from the finest grid. On the other hand the ECF requires for $\varepsilon = 10$ a finer discretization into $9,216$ panels to be within five percent of the finest grid result. For larger permittivities even the finest grid results of the ECF have not converged within reasonable accuracy.

Contrary to the equal potential case, the ECF provides accurate results for any permittivty ratio if the conductors are at different potentials. It can be seen from the table that all approximations using the $2,304$ panel grid are within one percent of the finest grid. This demonstrates that the bad scaling of the equal potential case is the sole source of error in the ECF.

C. Comparison with Modified Green's Function

The main purpose of the ECF and PA is to handle arbitrary distributions of dielectric materials. However, the case of layered media is common and modified Green's functions are an alternative to the ECF or PA. For a single dielectric interface at $x_3 = 0$ the Green's function can be found by the method of images

$$G_\varepsilon(x,x') = \begin{cases} \frac{1}{\varepsilon_0}\left(G(x,x') - \frac{\varepsilon_1-\varepsilon_0}{\varepsilon_0+\varepsilon_1}G(x,Px')\right), & x_3, x_3' > 0 \\ \frac{2}{\varepsilon_1+\varepsilon_0}G(x,x'), & x_3 \cdot x_3' < 0 \\ \frac{1}{\varepsilon_1}\left(G(x,x') - \frac{\varepsilon_0-\varepsilon_1}{\varepsilon_1+\varepsilon_0}G(x,Px')\right), & x_3, x_3' < 0 \end{cases}$$

where $G(x,x')$ is the free-space Green's function defined in (3) and Px is the image of x. Thus the capacitance problem reduces to solving

$$\int_{S_c} G_\varepsilon(x,x')\,\sigma_f(x')\,dS_{x'} = u(x), \quad x \in S_c \tag{23}$$

on the conductor surfaces.

In this example we consider two cubes above and below the interface as indicated in Figure 6 where $\varepsilon_0 = 1$.

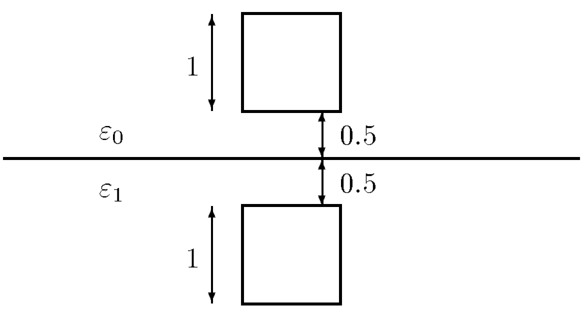

Fig. 6. Cross sectional view of two cubes in a layered medium

For the modified Green's function, each cube was discretized into 600 rectangular panels. In addition, for the ECF and PA the interface was truncated to a square plate of sidelength 12 and discretized into 784 panels.

Different from the case of a finite dielectric, only a potential that vanishes on the bottom conductor will generate a badly scaled density. If the potential is nonzero in the high-permittivity region, the charge density on the bottom conductor will not converge to zero as $\varepsilon_1 \to \infty$.

This suggests to use the PA only for the first column of the capacitance matrix. The results in Table III demonstrate that the capacitances calculated this way are in good agreement with the capacitances obtained from the modified Green's function approach. As expected, the ECF produces highly erroneous results when the permittivity ratio gets large.

If the top conductor is grounded and bottom conductor has a non-zero potential, then there is no bad scaling in the solution and the numerical approximation obtained by the ECF are in good agreement with those obtained by the modified Green's function appoach.

D. Bus Crossing

To demonstrate that the perturbation approach is also useful for complex multiconductor systems, the capacitance matrix associated with the bus-crossing structure of Figure 7 is calculated.

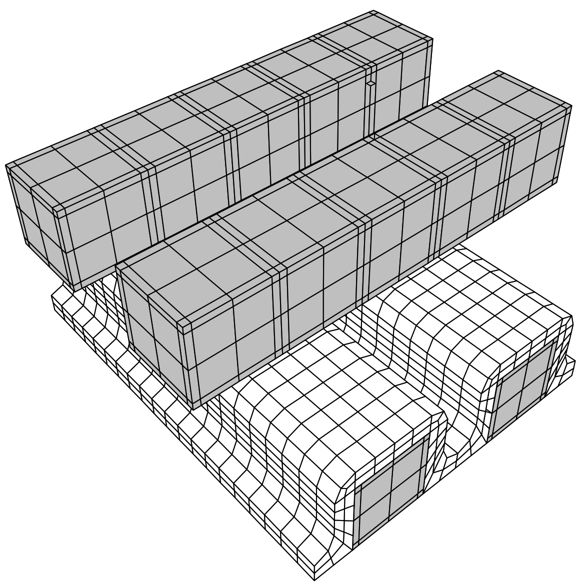

Fig. 7. Bus crossing example, the lower conductors are covered by a dielectric material. Discretization used in the calculations is finer than shown

All the conducting bars have 1×1 units cross-sections. Conductors 1 and 2 are covered by a dielectric material whose thickness is approximately 0.25

Panels	$\varepsilon = 10$ 576	2304	9216	36864	$\varepsilon = 100$ 576	2304	9216	36864	$\varepsilon = 1000$ 576	2304	9216	36864
$\mathbf{C}_{\mathrm{PA}}\begin{bmatrix}1\\1\end{bmatrix}$	8.018 5.109	8.623 5.496	8.893 5.675	9.025 5.765	8.567 5.544	9.307 6.034	9.652 6.273	9.826 6.396	8.627 5.592	9.384 6.096	9.738 6.341	9.917 6.469
$\mathbf{C}_{\mathrm{ECF}}\begin{bmatrix}1\\1\end{bmatrix}$	11.82 7.543	10.86 6.936	10.11 6.465	9.649 6.170	52.96 34.46	35.79 23.40	24.21 15.87	17.30 11.34	459.5 299.8	278.8 183.1	158.0 104.2	86.05 56.90
$\mathbf{C}_{\mathrm{ECF}}\begin{bmatrix}1\\-1\end{bmatrix}$	49.57 −45.35	50.58 −46.69	50.50 −46.87	50.29 −46.82	449.5 −431.7	454.9 −442.9	451.5 −443.4	448.0 −442.1	4446 −4293	4494 −4403	4457 −4406	4420 −4392

TABLE II

Convergence Behavior, Two Spheres in Ellipsoidal Dielectric Medium

	$p = [1,0]^T$ MG	PA	ECF	$p = [0,1]^T$ MG	ECF
$\varepsilon = 10$	11.94 −5.658	11.92 −5.639	11.86 −6.416	−5.658 68.42	−5.584 69.17
$\varepsilon = 100$	12.44 −6.162	12.43 −6.141	12.35 −15.31	−6.162 633.8	−6.073 642.8
$\varepsilon = 1000$	12.49 −6.218	12.48 −6.196	12.40 −99.42	−6.218 6282	−6.127 6374

TABLE III

Comparison of Capacitances for Figure 6 as calculated by modified Green's functions (MG), Perturbation Approach and Equivalent Charge Formulation.

units. The spacing between the conductors in horizontal direction is 0.4 units and 1 unit in vertical direction. The structure was discretized into $10,400$ panels, out of which $4,768$ panels were placed on the dielectric interface.

The capacitance matrices calculated by both methods are compared in Tables IV and Tables V. As expected, the results of both approaches are close for a small permittivity. The effect of the bad scaling in the ECF becomes obvious for the coupling capacitances between the top and bottom conductors when $\varepsilon_1 = 10$. The matrices of the ECF are not symmetric, even though a fine discretization was used. For the PA, the extend of the asymmetry is much smaller and does not grow when ε_1 is increased.

E. Connector

The capacitances associated with the backplane connector of Figure 8 are investigated in Table VI. For $\varepsilon_1 = 10$ the results of both methods appear to be close. However, the differences become obvious if the capacitance matrix is used to determine the net charges on the pins for a constant potential. From equation (8) it is clear that the net charges for this case must remain bounded in the limit $\varepsilon_1 \to \infty$. The results obtained by the perturbation approach reflect this behavior well, whereas the net charges of the equivalent charge formulation increase without bounds.

F. CPU Timing

The perturbation method involves solving an additional capacitance problem for the infinite permittivity case. Since this problem is always less complex than the original capacitance problem, the overall CPU time of the PA is less than twice the time of the ECF. The actual factor varies with the problem geometry and Table VII displays the timings for our examples. Our current implementation of the perturbation method restarts the whole calculation for the perturbation equation. Further optimizations could

$$\mathbf{C}_{\mathrm{ECF}} = \begin{bmatrix} 44.32 & -12.15 & -12.26 & -12.26 \\ -12.14 & 44.32 & -12.26 & -12.27 \\ -12.21 & -12.21 & 39.42 & -8.19 \\ -12.21 & -12.21 & -8.187 & 39.42 \end{bmatrix}$$

$$\mathbf{C}_{\mathrm{PA}} = \begin{bmatrix} 44.14 & -12.33 & -12.14 & -12.14 \\ -12.33 & 44.14 & -12.14 & -12.14 \\ -12.30 & -12.30 & 39.56 & -8.175 \\ -12.30 & -12.30 & -8.175 & 39.56 \end{bmatrix}$$

TABLE IV

Comparison of the calculated capacitance matrix for the bus crossing in Figure 7. Top: equivalent charge formulation; bottom: perturbation method. $\varepsilon_1 = 2$

$$\mathbf{C}_{\mathrm{ECF}} = \begin{bmatrix} 75.38 & -30.12 & -18.01 & -18.00 \\ -30.11 & 75.37 & -18.01 & -18.00 \\ -16.67 & -16.67 & 47.46 & -7.702 \\ -16.67 & -16.67 & -7.702 & 47.46 \end{bmatrix}$$

$$\mathbf{C}_{\mathrm{PA}} = \begin{bmatrix} 73.24 & -32.26 & -16.43 & -16.44 \\ -32.24 & 73.25 & -16.45 & -16.45 \\ -16.90 & -16.90 & 47.85 & -7.68 \\ -16.90 & -16.90 & -7.679 & 47.85 \end{bmatrix}$$

TABLE V

Comparison of the calculated capacitance matrices for the bus crossing in Figure 7. Top: equivalent charge formulation; bottom: perturbation method. $\varepsilon_1 = 10$

be achieved by re-using already calculated data of the infinite permittivity problem.

VIII. Conclusion

The capacitance calculation for structures with multiple dielectrics by the equivalent charge formulation can be erroneous when the ratio of the permittivities is high. The error is due to bad scaling of the solution and not due to ill-conditioning of the integral formulation. The perturbation approach described in this article does not suffer from an accuracy loss in this case. Furthermore, calculations with the new approach can be multipole-accelerated and are therefore efficient enough to allow capacitance extractions of complex three-dimensional, multiple-dielectric geometries.

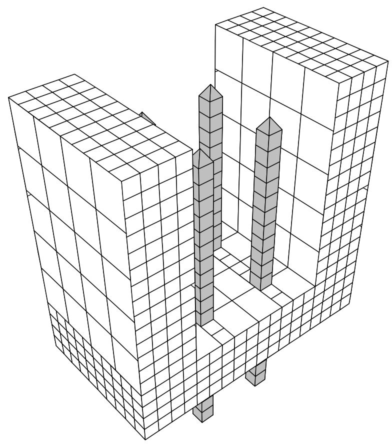

Fig. 8. Backplane Connector with four pins. Discretization used in the calculations is finer than shown.

$$\mathbf{C}_{\mathrm{ECF}} = \begin{bmatrix} 170.0 & -54.29 & -60.28 & -20.82 \\ -54.24 & 169.9 & -20.82 & -60.16 \\ -60.34 & -20.83 & 170.2 & -54.28 \\ -20.85 & -60.32 & -54.22 & 170.2 \end{bmatrix}$$

$$\mathbf{C}_{\mathrm{ECF}} \cdot \begin{bmatrix} 1 \\ 1 \\ 1 \\ 1 \end{bmatrix} = \begin{bmatrix} 34.65 \\ 34.71 \\ 34.72 \\ 34.80 \end{bmatrix}$$

$$\mathbf{C}_{\mathrm{PA}} = \begin{bmatrix} 168.1 & -56.21 & -62.20 & -22.73 \\ -56.17 & 168.0 & -22.74 & -62.09 \\ -62.28 & -22.77 & 168.2 & -56.22 \\ -22.79 & -62.27 & -56.17 & 168.2 \end{bmatrix}$$

$$\mathbf{C}_{\mathrm{PA}} \cdot \begin{bmatrix} 1 \\ 1 \\ 1 \\ 1 \end{bmatrix} = \begin{bmatrix} 26.98 \\ 27.01 \\ 26.96 \\ 27.02 \end{bmatrix}$$

TABLE VI

Comparison of the calculated capacitance matrices for the connector of Figure 8. $\varepsilon_1 = 10$

Finally, perturbation methods can also be applied to structures containing more than two dielectrics with high permittivity ratios, e.g. when $\varepsilon_0 = 1, \varepsilon_1 = 10$, and $\varepsilon_2 = 100$. However, the approach gets more involved, sometimes requiring the solution of two or more perturbation equations. Although it is fairly easy to tell what to do for a given structure, the description of the most general case appears to be hard and is beyond the scope of this paper.

	Sphere	Connector	Bus
# Panels	1,536	2,960	10,400
ECF	0:35	2:16	16:46
PA	0:45	3:16	25:42

TABLE VII
Total CPU times in minutes, $\varepsilon_1 = 10$

References

[1] R. F. Harrington, *Field Computation by Moment Methods.* New York: MacMillan, 1968.

[2] K. Nabors and J. White, "Fastcap: A multipole accelerated 3-D capacitance extraction program," *IEEE Trans. on Computer-Aided Design of Integrated Circuits and Systems*, vol. 11, no. 10, pp. 1447–1459, 1991.

[3] C. Wei, R. F. Harrington, J. R. Mautz, and T. K. Sarkar, "Multiconductor transmission lines in multilayered dielectric media," *IEEE Trans. Microwave Theory Tech.*, vol. 32, no. 4, pp. 439–449, 1984.

[4] K. Li, K. Atsuki, and T. Hasegawa, "General analytical solutions of static Green's functions for shielded and open arbitrary multilayered media," *IEEE Trans. Microwave Theory Tech.*, vol. 45, no. 1, pp. 2–8, 1997.

[5] V. Jandhyala, E. Michielssen, and R. Mittra, "Multipole-accelerated capacitance computation for 3-D structures in a stratified dielectric medium using a closed form Green's function," *int. J. Microwave and Millimeter-Wave Computer-Aided Eng.*, vol. 5, no. 2, pp. 68–78, 1995.

[6] S. Rao, T. Sarkar, and R. Harrington, "The electrostatic field of conducting bodies in multiple dielectric media," *IEEE Trans. Microwave Theory Tech.*, vol. 32, no. 11, pp. 1441–1448, 1984.

[7] K. Nabors and J. White, "Multipole-accelerated capacitance extraction algorithms for 3-D structures with multiple dielectrics," *IEEE Trans. Circuits and Systems*, vol. 39, no. 11, pp. 946–954, 1992.

[8] X. Cai, K. Nabors, and J. White, "Efficient Galerkin techniques for multipole-accelerated capacitance extraction of 3-D structures with multiple dielectrics," in *Proc. Conf. Advanced Research in VLSI*, (Chapel Hill), 1995.

[9] A. Ruehli and P. Brennan, "Efficient capacitance calculations for three-dimensional multiconductor systems.," *IEEE Trans. Microwave Theory Tech.*, vol. 2, no. 21, pp. 76–82, 1973.

[10] R. Kress, *Linear Integral Equations*, vol. 82 of *Applied Mathematical Sciences.* Berlin, Heidelberg, New York: Springer, 1989.

[11] V. Rokhlin, "Rapid solution of integral equations of classical potential theory," *J. Comput. Phys.*, vol. 60, no. 2, pp. 187–207, 1985.

[12] L. Greengard, *The Rapid Evaluation of Potential Fields in Particle Systems.* Cambridge, Massachusetts: MIT Press, 1988.